BIOLOGY OF REPRODUCTION (2015) **92**(3):63, 1–11
Published online before print 14 January 2015.
DOI 10.1095/biolreprod.114.123901

Roles of Toll-Like Receptors 2 and 4 in Mediating Experimental Autoimmune Orchitis Induction in Mice[1]

Zhenghui Liu,[3] Shutao Zhao,[3] Qiaoyuan Chen,[3] Keqin Yan,[3] Peng Liu,[3] Nan Li,[4] C. Yan Cheng,[4] Will M. Lee,[5] and Daishu Han[2,3]

[3]*Department of Cell Biology, Institute of Basic Medical Sciences, Chinese Academy of Medical Sciences, School of Basic Medicine, Peking Union Medical College, Beijing, China*
[4]*Center for Biomedical Research, The Population Council, New York, New York*
[5]*School of Biological Science, University of Hong Kong, Hong Kong, China*

ABSTRACT

The mammalian testis is an immunoprivileged site where male germ cell antigens are immunologically tolerated under physiological conditions. However, some pathological conditions can disrupt the immunoprivileged status and induce autoimmune orchitis, an etiological factor of male infertility. Mechanisms underlying autoimmune orchitis induction are largely unknown. The present study investigated the roles of Toll-like receptor 2 (TLR2) and TLR4 in mediating the induction of experimental autoimmune orchitis (EAO) in mice after immunization with male germ cell antigens emulsified with complete Freund adjuvant. Wild-type mice developed severe EAO after three immunizations, which was characterized by leukocyte infiltration, autoantibody production, and impaired spermatogenesis. *Tlr2* or *Tlr4* deficient mice showed relatively low susceptibility to EAO induction compared with wild-type mice. Notably, *Tlr2* and *Tlr4* double knockout mice were almost completely protected from EAO induction. Moreover, we demonstrated that TLR2 was crucial in mediating autoantibody production in response to immunization. The results imply that TLR2 and TLR4 cooperatively mediate EAO induction.

autoimmune orchitis, testis, Toll-like receptor

INTRODUCTION

During mammalian spermatogenesis, a large number of novel antigens are produced by developing germ cells after immunocompetence is established [1]. These antigens do not induce detrimental immune response within the testis under physiological conditions because of testicular immune privilege. However, some pathological conditions, such as infection, trauma, and inflammation, may overwhelm the immunosuppressive mechanisms and lead to chronic autoimmune orchitis, an etiological factor of male infertility [2]. Understanding the mechanisms underlying autoimmune orchitis development can aid in developing preventive and therapeutic strategies.

Experimental autoimmune orchitis (EAO) can be induced by immunizing rodent animals using allogeneic testicular antigens emulsified with adjuvants [3]. Some protocols may induce EAO without adjuvants in susceptible mouse strains [4]. EAO is characterized by the production of autoantibodies against germ cell antigens, local leukocyte accumulation, and proinflammatory cytokine upregulation within the testis, which can impair spermatogenesis and fertility [5]. EAO is usually induced by intervals of three immunizations and is a useful model to investigate the pathology of chronic autoimmune orchitis [6]. The critical role of $CD4^+$ lymphocytes in the pathogenesis of EAO has been established [7]. Proinflammatory cytokines, including tumor necrosis factor alpha (TNFA), interleukin 6 (IL6), and monocyte chemotactic protein 1 (MCP1), induce germ cell apoptosis and leukocyte infiltration in EAO [8]. However, the mechanisms mediating EAO formation remain to be fully understood.

Toll-like receptors (TLRs) belong to a family of pattern-recognition receptors that initiate innate immune responses to exogenous and endogenous stimuli [9]. Up to date, 10 human and 12 mouse TLRs have been identified. TLRs recognize conserved pathogen-associated molecular patterns (PAMPs) of microbial pathogens, and initiate innate immune responses against invading microbes [10]. For example, TLR2 recognizes bacterial peptidoglycan and lipopeptides [11, 12]. TLR4 recognizes lipopolysaccharides, the best-characterized PAMP that mediates pleiotropic effects on antigen-presenting cells [13]. TLRs are also activated by endogenous ligands that can be released from damaged tissues and necrotic cells, termed damage-associated molecular patterns, thereby inducing endogenous inflammatory responses [14]. Among the well-characterized damage-associated molecular patterns, high-mobility group box 1 (HMGB1) and several heat shock proteins (HSPs) are functional endogenous ligands of TLR2 and TLR4 [15–18]. TLR-initiated innate immune responses to microbial stimulation direct antigen-specific adaptive immune responses to prevent microbial infection [19]. TLR-initiated endogenous inflammatory responses are associated with autoimmune diseases [20, 21]. The mechanisms by which TLRs mediate the autoantigen-specific adaptive immunity remain unclear.

Recent studies demonstrated that different TLRs are critical in the induction of experimental autoimmune diseases, including experimental autoimmune encephalomyelitis (EAE) and experimental autoimmune uveitis (EAU) [22, 23]. The roles of TLRs in regulating testicular local immune defenses against microbial pathogens have been revealed [24]. The present study examined the involvement of TLR2 and TLR4 in mediating EAO induction.

[1]Supported by the National Natural Science Foundation of China (Grand Nos. 31171445, 31261160491, 31371518) and the Funds for Major State Basic Research Project of China (No. 2015CB94300).
[2]Correspondence: Daishu Han, PUMC & CAMS, 5 Dong Dan San Tiao, Beijing 100005, P.R. China. E-mail: dshan@ibms.pumc.edu.cn

Received: 31 July 2014.
First decision: 19 September 2014.
Accepted: 6 January 2015.

eISSN: 1529-7268 http://www.biolreprod.org
ISSN: 0006-3363

TABLE 1. Primers used for qRT-PCRs.

Target genes	Primer pairs (5′→3′)	
	Forward	Reverse
Il6	GAGGATACCACTCCCAACAGACC	AAGTGCATCATCGTTGTTCATACA
Tnfa	CATCTTCTCAAAATTCGAGTGACAA	TGGGAGTAGACAAGGTACAACCC
Mcp1	TTAACGCCCCACTCACCTGCTG	GCTTCTTTGGGACACCTGCTGC
Actb	GAAATCGTGCGTGACATCAAAG	TGTAGTTTCATGGATGCCACAG

MATERIALS AND METHODS

Animals

Tlr2 and *Tlr4* single-gene knockout ($Tlr2^{-/-}$ and $Tlr4^{-/-}$) mice with original genetic backgrounds of 50% C57BL/6 and 50% 129S1 were purchased from The Jackson Laboratories (Bar Harbor, ME). These mice were backcrossed to C57BL/6 for five generations. *Tlr2* and *Tlr4* double knockout ($Tlr2^{-/-}Tlr4^{-/-}$) and wild-type (WT) mice were produced by cross-mating $Tlr2^{-/-}$ and $Tlr4^{-/-}$ mice. Mice were inbred in a specific pathogen-free facility with nutrition (food and water ad libitum) and 12L:12D cycle. All the mice were handled in compliance with the Guideline for the Care and Use of Laboratory Animals approved by the Chinese Council on Animal Care.

Antibodies

Rabbit anti-CD163 (sc-33560, 1:100) and anti-IL6 (sc-1265-R, 1:100) were purchased from Santa Cruz Biotechnology (Santa Cruz, CA). Mouse anti-β-actin monoclonal antibody (A5316, 1:4000) was purchased from Sigma (St. Louis, MO). Rabbit anti-CD68 (ab125212, 1:100), anti-TNFA (ab34674, 1:100), anti-MCP1 (ab7202, 1:100), and rat anti-F4/80 (ab6640, 1:100) antibodies were purchased from Abcam (Cambridge, United Kingdom). Horseradish peroxidase (HRP)-conjugated secondary antibodies against mouse immunoglobulin G (IgG) (ZB-2305, 1:4000), rat IgG (ZB-2307), rabbit IgG (ZB-2301, 1:200) were purchased from Zhongshan Biotechnology Co. (Beijing, China). Phycoerythrin (PE)-conjugated anti-F4/80 antibody (123109, 1:200) was purchased from Biolegend (San Diego, CA). Fluorescein isothiocyanate (FITC)-conjugated anti-annexin V (556421, 1:100), PE-conjugated anti-CD3 (555275, 1:100), PE-Cy5-conjugated anti-CD4 (553050, 1:100), and PE-Cy5-conjugated anti-B220 (553091, 1:100) antibodies were purchased from BD Biosciences (San Jose, CA). PE-Cy5-conjugated anti-CD8 antibody (15–0081, 1:100) was purchased from eBioscience (San Diego, CA).

EAO Induction

Ten-week-old male mice were used for EAO induction based on a previously described protocol [25]. In brief, male germ cells from 10-wk-old mice were homogenized in 1× PBS. The homogenates were emulsified with an equal volume of complete Freund adjuvant (CFA) (Sigma). The emulsified homogenates of 10^8 cells in 0.4 ml were subcutaneously injected in three sites near the popliteal lymph nodes in each mouse. Mice that were injected with an equal volume of an emulsion of PBS with CFA alone served as the controls. Mice were immunized three times at an interval of 2 wk. The testes were collected for EAO analysis 50 days after the first immunization.

Histology and Immunohistochemistry

The testes were fixed in 10% neutral-buffered formalin for 24 h, embedded in paraffin, and cut into 5-μm thick sections. The paraffin sections were stained with hematoxylin-eosin and mounted with neutral balsam (Zhongshan Biotechnology Co.) for histological analysis under a microscope (BX51; Olympus, Tokyo, Japan). For immunohistochemistry, the testes were fixed in 4% paraformaldehyde for 24 h. After cryoprotection in 30% sucrose, the frozen sections were cut to a thickness of 7 μm using Leica CM1950 (Leica Biosystems, Nussloch, Germany). The sections were incubated with PBS containing 3% H_2O_2 for 10 min to inhibit endogenous peroxidase activity. After blocking with 5% rabbit serum in PBS for 1 h at room temperature, the sections were incubated with primary antibodies overnight at 4°C. The sections were washed three times with PBS, and incubated with HRP-conjugated secondary antibodies at room temperature for 30 min. HRP activity was visualized using the diaminobenzidine method based on the manufacturer's instructions. Negative controls were incubated with preimmune animal sera instead of primary antibodies. After being counterstained with hematoxylin, the sections were observed under the microscope.

Isolation of Testicular Interstitial Cells and Germ Cells

Testicular cells were isolated based on previously described procedures [26]. In brief, the testes were decapsulated and incubated with 0.5 mg/ml type I collagenase (Sigma) at room temperature for 15 min with gentle oscillation. Cell suspensions were passed through 80-μm copper meshes to remove the seminiferous tubules. The interstitial cells were collected by centrifugation at 600 × *g* for 10 min. After washing twice with ice-cold PBS, the cells were subjected to flow cytometry.

Male germ cells were isolated from 10-wk-old WT mice. After removal of the interstitial cells, the seminiferous tubules were cut into small pieces (~1 mm^3) and incubated with 0.5 mg/ml hyaluronidase (Sigma) at room temperature for 10 min with gently pipetting to dissociate the cells. The cell suspensions were filtered through 80-μm copper meshes, and the fraction of single cells was collected and homogenized in 1× PBS.

Isolation of Lymphocytes from the Renal Lymph Node

Mouse renal lymph nodes (RLNs) were removed and cut into small pieces in Hank balanced salt solution (Sigma). The suspensions were gently pipetted to dissociate cells, and filtered through 80-μm copper meshes. The single-cell fractions were collected for flow cytometry.

Flow Cytometry

Flow cytometry analysis was performed according to the antibody manufacturer's instructions. Briefly, testicular interstitial cells and RLN lymphocytes were freshly isolated. To label cell markers, 1×10^6 cells in 50 μl PBS containing 3% bovine serum albumin were incubated on ice for 30 min with annexin V and appropriate specific antibodies or isotype controls. The cells were analyzed using FACSCanto flow cytometer (BD Biosciences).

Real-Time Quantitative RT-PCR

Total RNA was extracted from the testis using TRIzol reagent (Life Technologies, Carlsbad, CA). RNA was treated with RNase-free DNase I (Life Technologies) to remove genomic DNA contamination. The absence of genomic DNA was confirmed by amplification of β-actin (*Actb*) using RNA without reverse transcription. RNA (1 μg) was reverse transcribed into cDNA in a 20 μl reaction system containing 2.5 μM random hexamers, 2 mM deoxynucleotidyl triphosphates, and 200 units Moloney murine leukemia virus reverse transcriptase (Promega, Madison, WI). PCR was performed in 20 μl of reaction system containing 0.2 μl of cDNA, 0.5 μM each of forward and reverse primers, and 10 μl of 2× Power SYBR Green PCR Master Mix kit (Life Technologies) using an ABI PRISM 7300 real-time cycler (Applied Biosystems, Foster City, CA). Relative mRNA levels of target genes normalized to *Actb* were obtained using the $2^{-\Delta\Delta Ct}$ formula described in Applied Biosystems User Bulletin No. 2 (P/N 4303859). Reaction efficiencies were between 92% and 100% for all amplifications. The primer sequences are listed in Table 1.

Enzyme-Linked Immunosorbent Assay

Testes were lysed by grinding in 1× PBS and centrifuged at 800 × *g* for 5 min. The cytokine levels in the supernatants were measured using enzyme-linked immunosorbent assay (ELISA) kits according to the manufacturer's instructions. ELISA kits for TNFA (BMS607/3), IL6 (BMS603/2), and MCP1 (BMS6005) were purchased from eBioscience. For all ELISA kits, the limit of

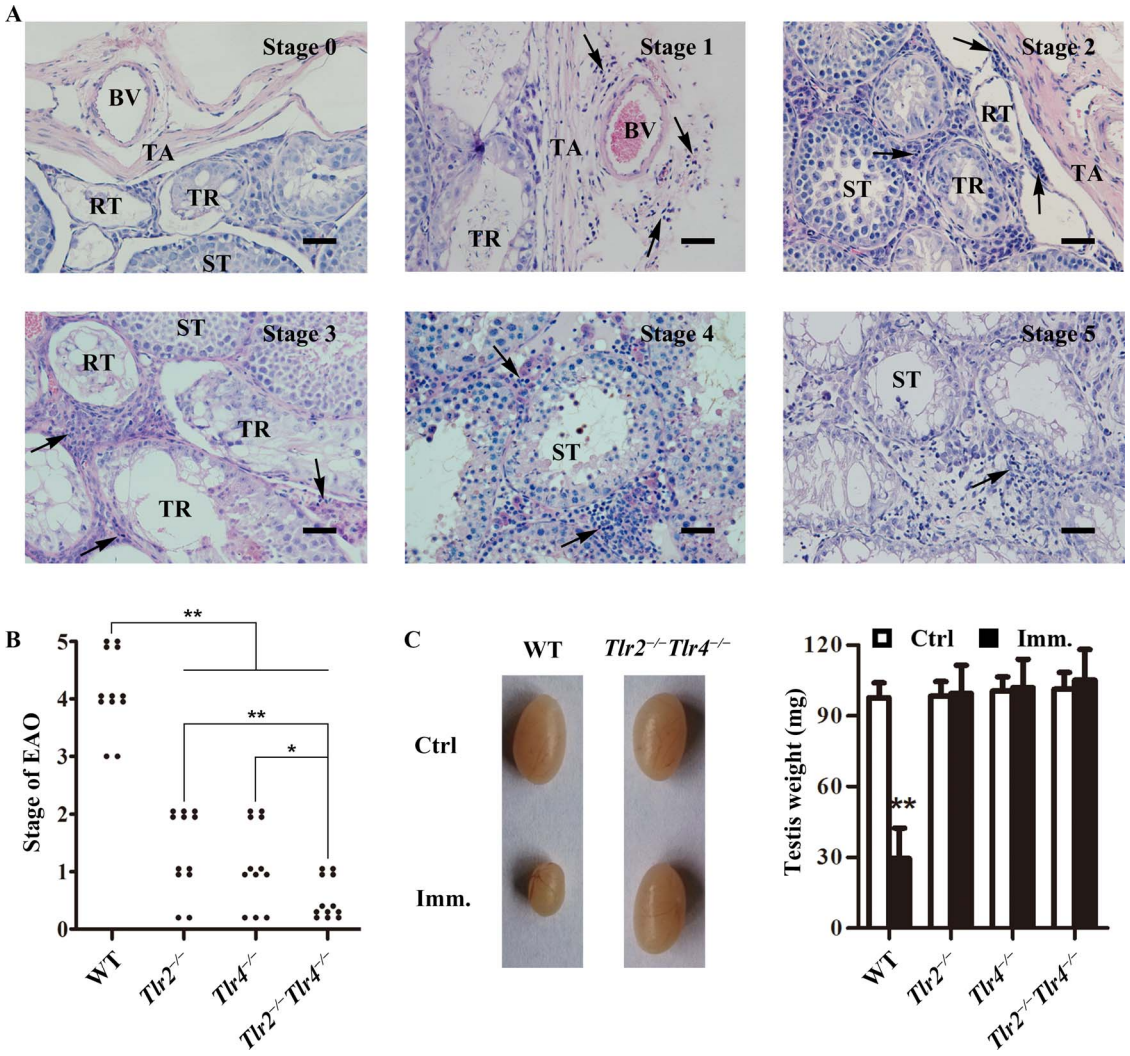

FIG. 1. EAO score. **A**) Histological EAO score. Paraffin sections of the testes were stained with hematoxylin-eosin. Images represent six stages of testicular inflammation. Arrows, focal inflammation; BV, blood vessel; RT, rete testis; ST, seminiferous tubule; TR, tubuli recti; TA, tunica albuginea. Bar = 20 μm. **B**) EAO stages. Mice with indicated genotypes were immunized three times with male germ cell homogenates emulsified in CFA. At 50 days after the first immunization, EAO stages were evaluated based on histological score. Twelve mice were analyzed in each group. **C**) Testis size. Representatives of the testicular size in wild-type (WT) and $Tlr2^{-/-}Tlr4^{-/-}$ mice 50 days after the first immunization (Imm). Mice injected with CFA alone served as the control (Ctrl). Testis weight was measured in the indicated mice (right panel). Data represent mean values ± SEM (n = 12). EAO score severity was statistically analyzed using the Kruskal-Wallis test. $^{*}P < 0.05$, $^{**}P < 0.01$.

detection was less than 10 pg/ml, and intra- and interassay variation were <5% and <10%, respectively.

Western Blot Analysis

Testes were lysed using lysis buffer (C1053; Applygen Technologies Inc., Beijing, China). Protein concentration was determined using a bicinchoninic acid protein assay kit (Pierce Biotechnology, Rockford, IL). Equal amount of proteins (20 μg/lane) were separated on 10% SDS-PAGE gel and subsequently electrotransferred onto polyvinyl difluoride membranes (Millipore, Bedford, MA). The membranes were blocked in Tris-buffered saline (25 mM TBS, pH7.4, 130 mM NaCl) containing 5% nonfat milk for 1 h, and then incubated with mouse sera overnight at 4°C. The membranes were washed three times with Tris-buffered saline containing 0.1% Tween-20 and incubated with HRP-conjugated anti-mouse IgG (Zhongshan Biotechnology Co.) at room temperature for 1 h. HRP activity was detected using an enhanced chemiluminescence detection kit (Santa Cruz, CA).

Biotin Tracing Assay

The permeability of the blood-testis barrier (BTB) was assessed by biotin tracer assay as previously described [27]. The mice were anesthetized with 50 mg/kg body weight pentobarbital sodium. Approximately 20 μl of 10 mg/ml EZ-link Sulfo-NHS-LC-Biotin (Thermo Scientific, Rockford, IL) was injected underneath of the testicular capsule using a 30-gauge needle. After 30 min, the testes were recovered. The paraffin sections were stained with FITC-conjugated streptavidin (Vector Laboratories, Burlingame, CA) at room temperature for 30 min. Subsequently, the sections were counterstained with 4′,6-diamidino-2-phenylindole (DAPI) for 10 min. Slides were mounted with neutral balsam for observation under the microscope (BX51; Olympus).

Statistical Analysis

Data represent the mean ± standard error of the mean (SEM). Statistical significance was determined using the Student *t* test. The calculations were performed using statistical software SPSS version 13.0 (SPSS Inc., Chicago, IL). $P < 0.05$ was considered statistically significant.

RESULTS

EAO Score

To determine the involvement of TLR2 and TLR4 in mediating EAO induction, $Tlr2^{-/-}$, $Tlr4^{-/-}$, $Tlr2^{-/-}Tlr4^{-/-}$, and WT mice were immunized with male germ cell

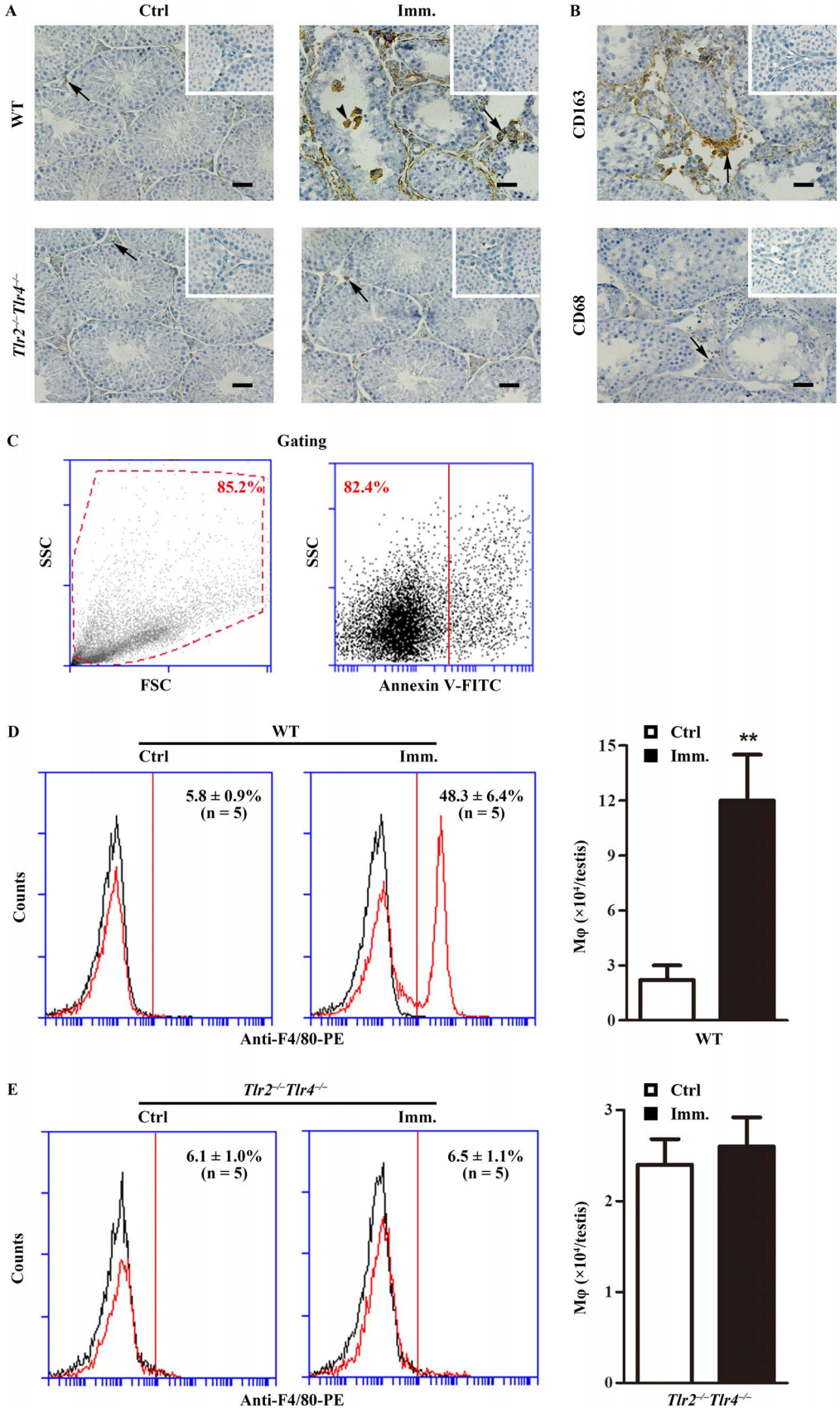

FIG. 2. Macrophage accumulation. **A**) Immunohistochemistry for macrophages. Testicular cryosections of WT and *Tlr2*$^{-/-}$*Tlr4*$^{-/-}$ mice at 50 days after the first immunization (Imm.) were immunostained with anti-F4/80 antibody (right panels). Testes of mice injected with CFA alone served as control (Ctrl, left panels). **B**) Detection of CD163^{+} and CD68^{+} cells. Immunohistochemical analyses of testicular sections of immunized WT mice were performed using specific antibodies against CD163 and CD68. Insets in the upper right corner are the negative controls in which preimmune sera were used as primary antibodies. Arrows and arrowheads indicate macrophages in the interstitial spaces and seminiferous tubules. Bar = 20 μm. The images are the

homogenates emulsified with CFA. EAO was analyzed 50 days after the first immunization based on previously described scales [4]. EAO was scored based on six stages (Fig. 1A): stage 0, no detectable inflammation in the testis; stage 1, focal inflammation (arrows) in the tunica albuginea; stage 2, focal inflammation adjacent to the tubuli recti; stage 3, inflammation surrounding the tubuli recti; stage 4, inflammation spreading around the seminiferous tubules and mild damage of the seminiferous epithelium; and stage 5, severe inflammation surrounding the tubules and damage of the seminiferous epithelium. The immunization induced EAO of stages 3–5 in all WT mice (Fig. 1B). Mild EAO of stages 1 and 2 also developed in *Tlr2*$^{-/-}$ and *Tlr4*$^{-/-}$ mice after immunization. By contrast, only four EAO cases of stage 1 were found in 12 *Tlr2*$^{-/-}$*Tlr4*$^{-/-}$ mice. In agreement with EAO severity, the testis weight significantly decreased in immunized WT mice, but did not change in *Tlr2*$^{-/-}$, *Tlr4*$^{-/-}$, and *Tlr2*$^{-/-}$*Tlr4*$^{-/-}$ mice (Fig. 1C). In the controls, the injection of WT mice with CFA or germ cell lysates alone did not induce EAO (data not shown).

Immune Cell Infiltration

Accumulation of immune cells, including macrophages and lymphocytes, in the testis is a hallmark of EAO [7, 28]. Immunohistochemistry using antibodies against F4/80 (a macrophage marker) showed evident accumulation of macrophages in the testicular interstitial spaces (arrows) of WT mice after immunization compared with that in the controls (Fig. 2A, upper panels). Macrophages were occasionally observed within the seminiferous tubules (arrowhead). By contrast, only a few macrophages were detected in the testes of control and immunized *Tlr2*$^{-/-}$*Tlr4*$^{-/-}$ mice (Fig. 2A, lower panels). Macrophages in the testes of immunized WT mice were predominantly CD163^{+} (Fig. 2B, upper panel), which represent infiltrated circulating macrophages. By contrast, the number of CD68^{+} macrophages, which represent testicular resident macrophages, remained low (Fig. 2B, lower panel). Total macrophage numbers in the testes were determined by flow cytometry after gating out cell debris and apoptotic cells (Fig. 2C). More than 4-fold increase in macrophages was detected in the testes of WT mice after immunization (Fig. 2D, right panel). However, immunization did not significantly affect the testicular macrophage numbers in *Tlr2*$^{-/-}$*Tlr4*$^{-/-}$ mice (Fig. 2E).

The lymphocyte numbers in the EAO testes were determined by flow cytometry. Cell debris and apoptotic cells were gated out (Fig. 3A). CD3^{+}CD4^{+} (Fig. 3B) and CD3^{+}CD8^{+} (Fig. 3C) T lymphocytes significantly increased in the testes of WT mice after immunization. Notably, absolute numbers of CD3^{+}CD4^{+} cells per testis were about 4-fold more than those of CD3^{+}CD8^{+} cells. By contrast, immunization did not induce B lymphocyte infiltration (Fig. 3D).

Lymphocyte Expansion in RLN

To further analyze the response of lymphocyte cells to immunization, we examined lymphocyte expansion in RLN. The RLN in WT mice were markedly enlarged 50 days after the first immunization (Fig. 4A). Immunization did not apparently change the RLN size in *Tlr2*$^{-/-}$*Tlr4*$^{-/-}$ mice. Lymphocyte subsets in RLN were determined by flow cytometry after gating out debris and apoptotic cells (Fig. 4B, upper left panels). The percentage of CD3^{+}CD4^{+} cells significantly increased in the RLN of WT mice after immunization (Fig. 4B, upper right panels). Absolute CD3^{+}CD4^{+} cell numbers per RLN were dramatically increased in immunized WT mince (Fig. 4B, upper right panel). By contrast, the ratios of CD3^{+}CD8^{+} cells and B cells slightly decreased although the absolute cell numbers significantly increased in the RLN of immunized WT mice (Fig. 4B, lower panels). The lymphocyte subsets remained consistent in the RLN of *Tlr2*$^{-/-}$*Tlr4*$^{-/-}$ mice after immunization (Fig. 4C). These results suggest that immunization predominantly expanded CD3^{+}CD4^{+} T cells in the RLN of WT mice.

Expression of Inflammatory Cytokines

The upregulation of proinflammatory cytokines, including IL6, TNFA, and MCP1, in the testis is involved in EAO pathogenesis [8]. Real-time quantitative RT-PCR (qRT-PCR) showed that the *Tnfa, Il6,* and *Mcp1* mRNA levels were dramatically upregulated in the testis of WT mice after immunization (Fig. 5A). By contrast, immunization faintly increased the cytokine mRNAs in the testis of *Tlr2*$^{-/-}$*Tlr4*$^{-/-}$ mice. ELISA results confirmed that the cytokine levels in the testis significantly increased in WT mice after immunization (Fig. 5B, left panel), but those in *Tlr2*$^{-/-}$*Tlr4*$^{-/-}$ mice did not change (Fig. 5B, right panel). Immunohistochemistry showed that TNFA was predominantly localized in Sertoli cells (arrows) in the testis of control WT mice (Fig. 5C, left upper panel). IL6 and MCP1 were not detected by immunohistochemistry in the controls. By contrast, evident increased signals of TNFA, IL6, and MCP1 were detected in the testes of immunized WT mice (Fig. 5C, right panels). Notably, all three cytokines were detected in Sertoli cells (arrows) and interstitial cells (arrowheads).

Autoantibody Production

The production of autoantibodies against germ cell antigens is another hallmark of EAO [5]. Western blot results showed that the sera of WT mice 50 days after immunization recognized multiple germ cell antigens with molecular weights between 30 to 100 kDa (Fig. 6A, left panels). Only low levels of antibodies against antigens around 30 and 75 kDa were detected in *Tlr2*$^{-/-}$ mice. Major antibodies that recognize ~100 kDa antigens disappeared in *Tlr2*$^{-/-}$ mice. However, the antibodies recognizing germ cell antigens of around 30, 40, 55, and 100 kDa were produced in immunized *Tlr4*$^{-/-}$ mice. The autoantibodies were not evident in the sera of immunized *Tlr2*$^{-/-}$*Tlr4*$^{-/-}$ mice (Fig. 6A, right panels). We did not detect

representatives of at least three mice. Immunohistochemistry was performed on one testis in each mouse. **C**–**E**) Quantitative analysis of macrophages. Testicular interstitial cells were labeled with FITC-conjugated annexin V (annexin V-FITC, a marker of apoptotic cells) and PE-conjugated anti-F4/80 antibody (anti-F4/80-PE). Cell debris (**C**, left panel) and apoptotic cells (**C**, right panel) were gated out. Flow cytometry density plots are the representatives of the interstitial cells from immunized WT mice. Macrophages in the testes of WT (**D**) and *Tlr2*$^{-/-}$*Tlr4*$^{-/-}$ (**E**) mice were quantitatively analyzed using flow cytometry. Left panels represent flow cytometry density plots, and right panels represent absolute macrophage numbers per testis based on flow cytometry data. Data are mean values ± SEM of five mice. Two testes per mouse were used in each flow cytometry analysis. $^{**}P < 0.01$.

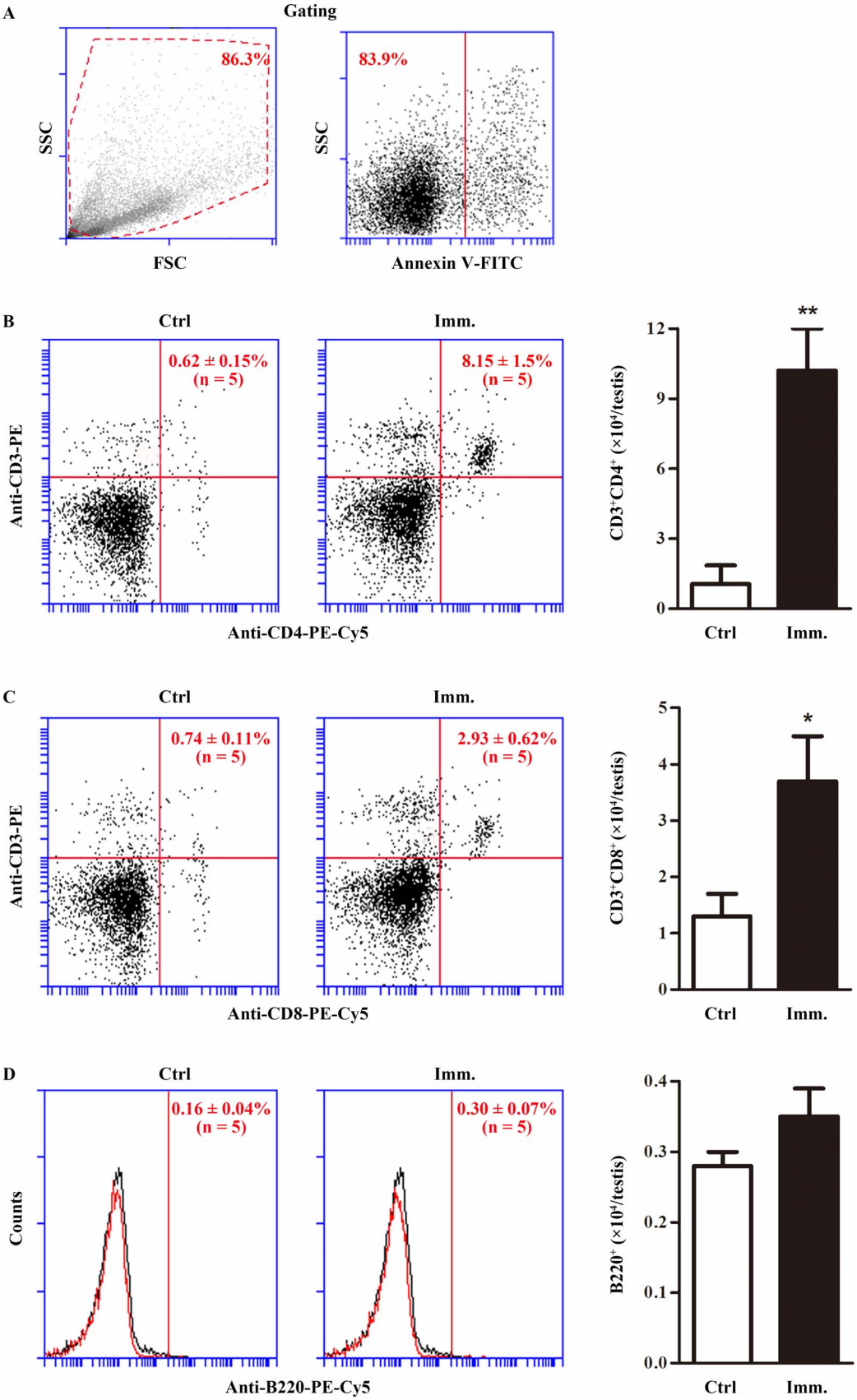

FIG. 3. Testicular lymphocytes. Testicular interstitial cells were isolated from the testis of control (Ctrl) and immunized (Imm.) WT mice. **A**) Cell gating. The interstitial cells were labeled with annexin V-FITC and appropriate antibodies. Cell debris (left panel) and apoptotic cells (right panel) were gated out. Flow cytometry density plots are the representatives of the interstitial cells from immunized WT mice. **B**) $CD4^+$ T lymphocytes. Testicular interstitial cells were labeled with annexin V-FITC, PE-conjugated anti-CD3 (anti-CD3-PE), and PE-Cy5-conjugated anti-CD4 antibodies (anti-CD4-PE-Cy5). After gating out cell debris and apoptotic cells, $CD3^+CD4^+$ T cells were analyzed by flow cytometry (left and middle panels). Absolute numbers of $CD3^+CD4^+$ cells

the autoantibodies in all the control mice. These results suggest that TLR2 plays a critical role in mediating the production of autoantibodies against male germ cell antigens. Immunohistochemistry confirmed that different stages of germ cells were stained by the sera of WT and *Tlr4*$^{-/-}$ mice 50 days after immunization (Fig. 6B). By contrast, the sera of immunized *Tlr2*$^{-/-}$ and *Tlr2*$^{-/-}$*Tlr4*$^{-/-}$ mice did not stain germ cells (data not shown). Moreover, the autoantibodies were deposited in male germs cells in immunized WT mice (Fig. 6C, left panel). We did not observe the autoantibody deposits in the testis of immunized *Tlr4*$^{-/-}$ mice (Fig. 6C, right panel) as well as immunized *Tlr2*$^{-/-}$ and *Tlr2*$^{-/-}$*Tlr4*$^{-/-}$ mice (data not shown).

Permeability of BTB

Autoantibody deposits in male germ cells of immunized WT mice suggest that BTB permeability was defective. Biotin tracing assay showed that biotin accessed the adluminal compartments (asterisks) of the seminiferous tubules in WT mice after immunization (Fig. 7, upper panels). By contrast, biotin was only detected in the basal membranes (arrows) and interstitial spaces (arrowheads) of the testes in the control mice (Fig. 7, lower panels). We did not detect biotin diffusion into the adluminal compartments of the seminiferous tubules in *Tlr2*$^{-/-}$, *Tlr4*$^{-/-}$, and *Tlr2*$^{-/-}$*Tlr4*$^{-/-}$ mice after immunization (data not shown).

DISCUSSION

Although the testis is an immunoprivileged site that prevents detrimental immune responses to immunogenic male germ cells under physiological conditions, some pathological stimuli may induce immune responses against male germ cell antigens and lead to autoimmune orchitis, thereby perturbing male fertility [29]. However, the mechanisms underlying the induction of autoimmune orchitis remain unclear. This study demonstrated the roles of TLR2 and TLR4 in mediating EAO induction.

EAO is a useful model to study the pathogenesis of chronic autoimmune orchitis [30]. EAO can be induced by three intervals of immunizations of rats with testicular autoantigens [31]. Single or two immunizations in the presence or absence of adjuvants may induce EAO in some susceptible mouse strains, but not in C57BL/6 mice [30]. Accordingly, these protocols do not induce EAO in mice used in the present study (data not shown). Therefore, we adopted immunization procedures for rats in the present study. We showed that three 2-wk-interval immunizations of WT mice with allogeneic male germ cell homogenates emulsified in CFA induced evident EAO at 50 days after the first immunization. By contrast, immunization only induced mild EAO in *Tlr2*$^{-/-}$ or *Tlr4*$^{-/-}$ mice. Remarkably, EAO was not evidently induced in *Tlr2*$^{-/-}$ *Tlr4*$^{-/-}$ mice. Although EAO in WT mice was more severe at prolonged time points, *Tlr2*$^{-/-}$*Tlr4*$^{-/-}$ never developed evident EAO (data not shown). These results indicate that TLR2 and TLR4 cooperatively played critical roles in mediating EAO induction.

TLRs initiate innate immune responses after recognition of PAMPs of most microbes, including bacteria, viruses, fungi, and parasites [32]. TLRs can also be activated by numerous endogenous agonists that are released from damaged tissues and necrotic cells. For example, HMGB1 and several HSPs, which are abundantly expressed in male germ cells, induce endogenous inflammatory responses through TLR2 and TLR4 [33–37]. TLR-initiated innate immune responses in innate immune cells facilitate antigen-specific adaptive immune responses by modulating lymphocyte proliferation and differentiation [19]. Notably, TLR2 and TLR4 are also expressed and functional in B cells [38]. The investigation on the potential role of TLRs in autonomously regulating B cell response in EAO would provide further insights into the mechanisms that utilize TLR2 and TLR4 in mediating EAO induction. In the present study, we demonstrated that immunization of WT mice induced the production of antibodies recognizing multiple germ cell antigens with molecular weights between 30 to 100 kDa. This result suggests that multiple germ cell antigens could induce autoimmune responses in EAO mice. Identification of the antigens that induce autoantibody production would expand our understanding of the mechanisms underlying autoimmune orchitis.

Although both TLR2 and TLR4 were required for evident EAO induction, they could play different roles in mediating EAO formation. Notably, TLR2 was critical for autoantibody production because the autoantibodies were significantly reduced in immunized *Tlr2*$^{-/-}$ mice. By contrast, *Tlr4* deficiency did not apparently affect autoantibody production. However, we did not detect autoantibody deposits in immunized *Tlr4*$^{-/-}$ mice. This result could be due to the fact that BTB permeability did not change in *Tlr4*$^{-/-}$ mice after immunization. Thus, autoantibody production in *Tlr4*$^{-/-}$ mice did not lead to severe EAO. This observation corresponds to the view that autoimmune orchitis is a cell-mediated immune disease [3]. In the present study, we demonstrated that immunization of WT mice dramatically induced macrophage and T lymphocyte infiltration into the testis. These results were in agreement with the fact that T lymphocytes are involved in the pathogenesis of many tissue-specific autoimmune diseases [39]. An early study showed that CD4$^+$ cells play critical roles in EAO pathogenesis in rats [40]. Accordingly, CD4$^+$ cell response was prominent in this study.

Macrophage infiltration and proinflammatory cytokines produced by macrophages are hallmarks of EAO, and they are involved in pathogenesis [8]. Our results demonstrated evident accumulation of CD163$^+$ macrophages, which represent infiltrated macrophages, in the testis of WT mice after immunization. By contrast, the number of testicular resident macrophages, which are marked by CD68, remained consistent. These results are in agreement with the observations in rat EAO [28]. Moreover, TNFA, IL6, and MCP1 levels in the testis significantly increased in WT mice after immunization. TNFA and IL6 induce germ cell apoptosis [41, 42]. MCP1 can promote leukocyte infiltration into the testis [43]. TNFA, IL6, and MCP1 were detected not only in testicular interstitial cells, but were also markedly upregulated in Sertoli cells. The upregulation of the proinflammatory cytokines in Sertoli cells could be a secondary effect of damaged germ cells. This hypothesis is supported by our recent demonstration that damaged male germ cells induce the expression of these three

per testis were calculated based on flow cytometry data (right panel). **C**) CD8$^+$ T cells. Testicular interstitial cells were labeled with annexin V-FITC, anti-CD3-PE, and PE-Cy5-conjugated anti-CD8 (anti-CD8-PE-Cy5) antibodies. CD3$^+$CD8$^+$ T cells were analyzed using flow cytometry. **D**) B cells. Cells were analyzed after labeling with annexin V-FITC and PE-Cy5-conjugated anti-B220 antibodies (anti-B220-PE-Cy5). Flow cytometry density plots represent five mice. Two testes per mouse were used in each flow cytometry analysis. Data are mean values ± SEM of five mice. *$P < 0.05$, **$P < 0.01$.

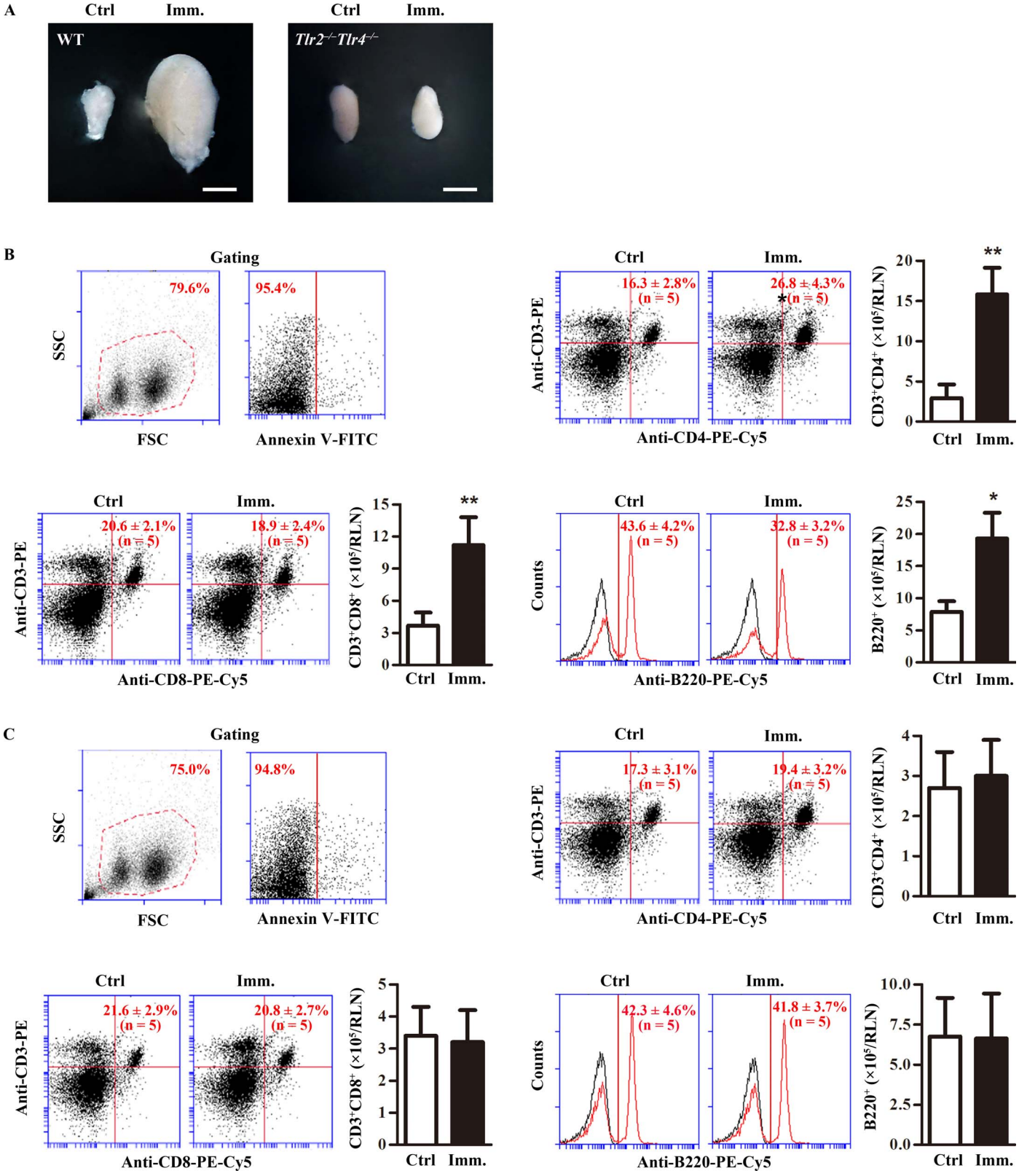

FIG. 4. Lymphocytes in renal lymph node (RLN). **A**) RLN size. WT and *Tlr2*$^{-/-}$*Tlr4*$^{-/-}$ mice were immunized. At 50 days after the first immunization (Imm.), RLNs were collected. Images are the representatives of the RLNs of five mice. Bar = 1 mm. **B**) Lymphocytes in the RLNs of WT mice. RLN cells were isolated from control (Ctrl) and immunized WT mice. Cells were labeled with annexin V-FITC and appropriate antibodies. Cell debris and apoptotic cells were gated out (upper left panels). Ratios and absolute numbers of $CD3^+CD4^+$ T cells (upper right panels), $CD3^+CD8^+$ T cells (lower left panels), and B cells (lower right panels) were determined using flow cytometry. **C**) Lymphocytes in RLNs of *Tlr2*$^{-/-}$*Tlr4*$^{-/-}$ mice. RLN cells were isolated from control and immunized *Tlr2*$^{-/-}$*Tlr4*$^{-/-}$ mice. Cells were analyzed as in **B**. Data are mean values ± SEM of five mice. Two RLNs per mouse were used in each flow cytometry analysis $^{**}P < 0.01$.

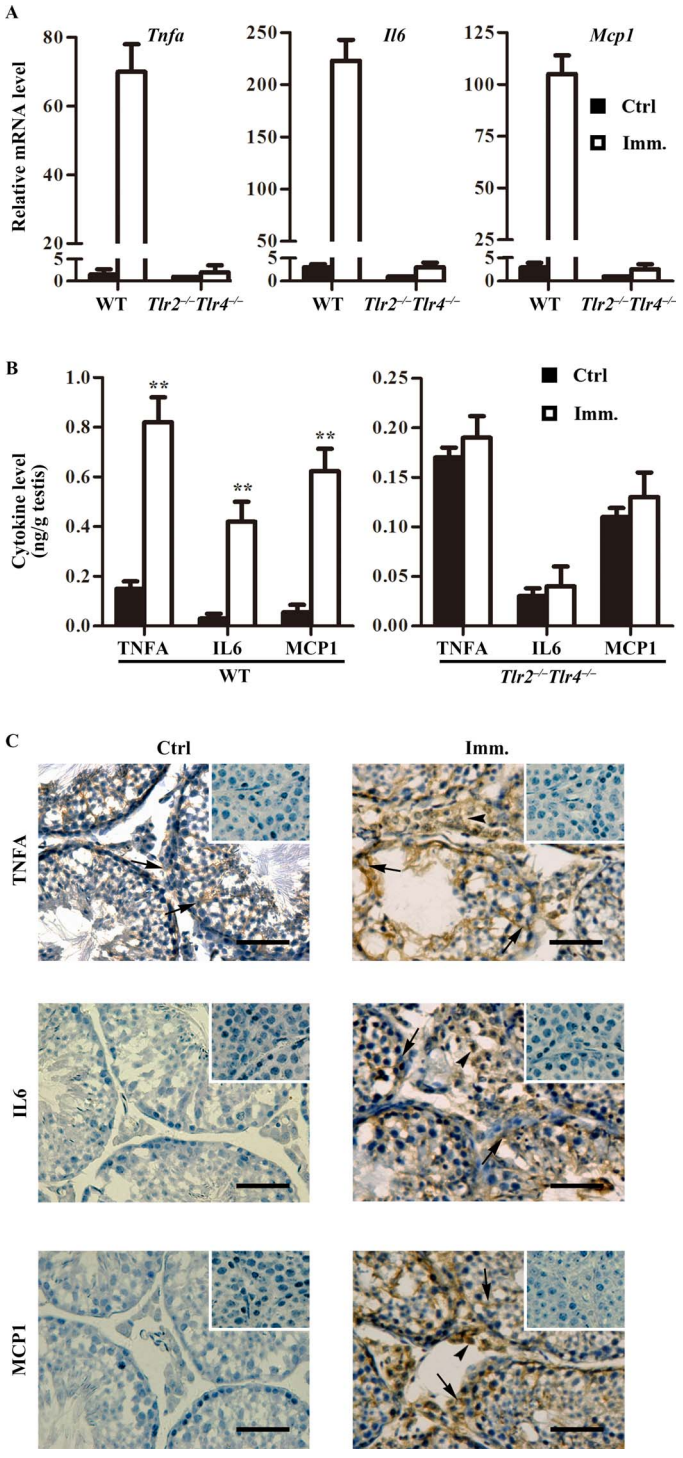

FIG. 5. Expression of proinflammatory cytokines in the testis. **A**) Relative mRNA levels of cytokines. Total RNAs were extracted from testes of control and immunized WT and *Tlr2*$^{-/-}$*Tlr4*$^{-/-}$ mice. Relative mRNA levels of major proinflammatory cytokines, including *Tnfa, Il6,* and *Mcp1,* were determined using real-time qRT-PCR normalized to β-*actin*. **B**) Protein levels of cytokines in the testis. Testes were lysed in PBS. The cytokine levels in the testis lysates of WT (left panel) and *Tlr2*$^{-/-}$*Tlr4*$^{-/-}$ (right panel) mice were measured using ELISA. **C**) Cellular distribution of cytokines in the testis. Immunohistochemistry on the cryosections of testes from control (Ctrl; left panels) and immunized (Imm.; right panels) WT mice was performed using antibodies against TNFA, IL6, and MCP1. Insets in the upper right corner are the negative controls in which preimmune sera were used as primary antibodies. Arrows and arrowheads indicate Sertoli cells and interstitial cells, respectively. Images represent at least three independent experiments on three mice. Bar = 20 μm. Data represent mean values ± SEM of three experiments. $^{**}P < 0.01$

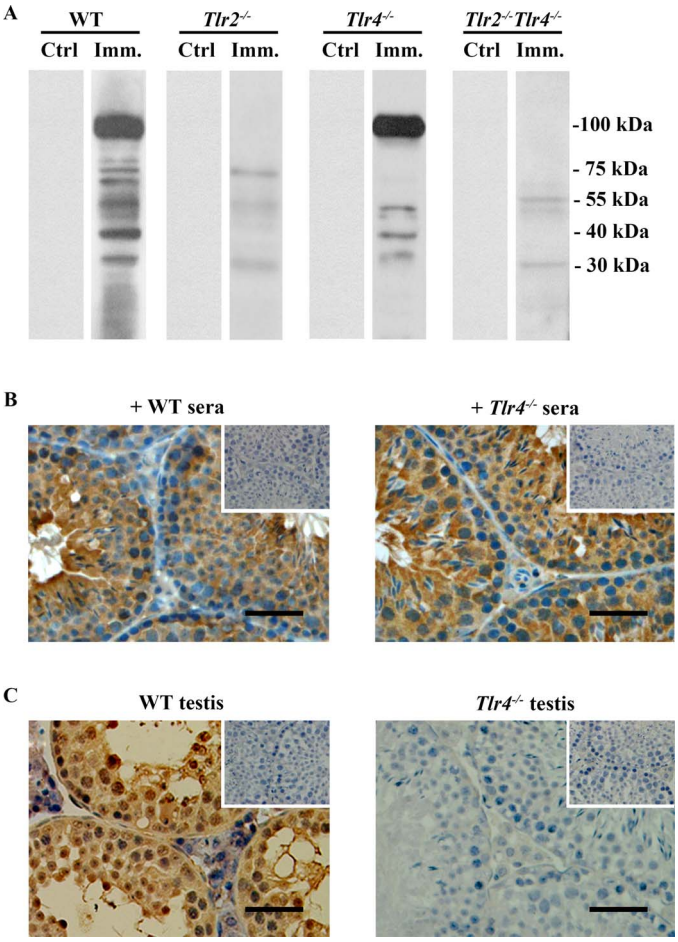

FIG. 6. Autoantibody production. **A**) Autoantibodies in sera. Male germ cells were isolated from 10-wk-old WT mice. Western blot analysis on the germ cell lysates was performed using sera (1:500 dilution) of WT, *Tlr2*$^{-/-}$, *Tlr4*$^{-/-}$, and *Tlr2*$^{-/-}$*Tlr4*$^{-/-}$ mice 50 days after the first immunization (Imm.) as the primary antibodies. The sera of mice that were injected with CFA alone served as controls (Ctrl). **B**) Distribution of autoantibodies. Testicular sections of 10-wk-old WT mice were immunostained with sera (1:100 dilution) of immunized WT (left panel) and *Tlr4*$^{-/-}$ (right panel) mice as the primary antibody. Insets in the upper right corners are negative controls in which the sera of control mice were used as the primary antibodies. **C**) Autoantibody deposition. Testicular sections of immunized WT (left panel) and *Tlr4*$^{-/-}$ (right panel) mice were directly stained with anti-mouse IgG antibodies. Signals in germ cells of WT mice indicate deposition of antibodies against germ cell antigens. Testes of the control mice served as the negative control (insets in upper right corners). Images are representatives of at least three mice. One testis in each mouse was used for immunostaining. Bar = 20 μm.

inflammatory cytokines in mouse Sertoli cells through the activation of TLR2 and TLR4 [44].

EAO is usually induced by the testicular autoantigens emulsified in CFA containing *Mycobacterium tuberculosis* in rats. Both TLR2 and TLR4 can be activated by *M. tuberculosis* and initiate an immune response [45]. CFA is also necessary for the induction of other experimental autoimmune disease, such as EAE and EAU [46, 47]. The CpG motif oligonucleotide (a TLR9 agonist) and *Bordetella pertussis* can also be adjuvants for experimental autoimmune disease induction [22, 48]. These observations suggest that adjuvant-triggered innate immune responses promote the induction of autoantigen-specific autoimmune diseases. Accordingly, we recently demonstrated that negative regulators of innate immune response inhibit EAO induction [49]. The mechanisms by

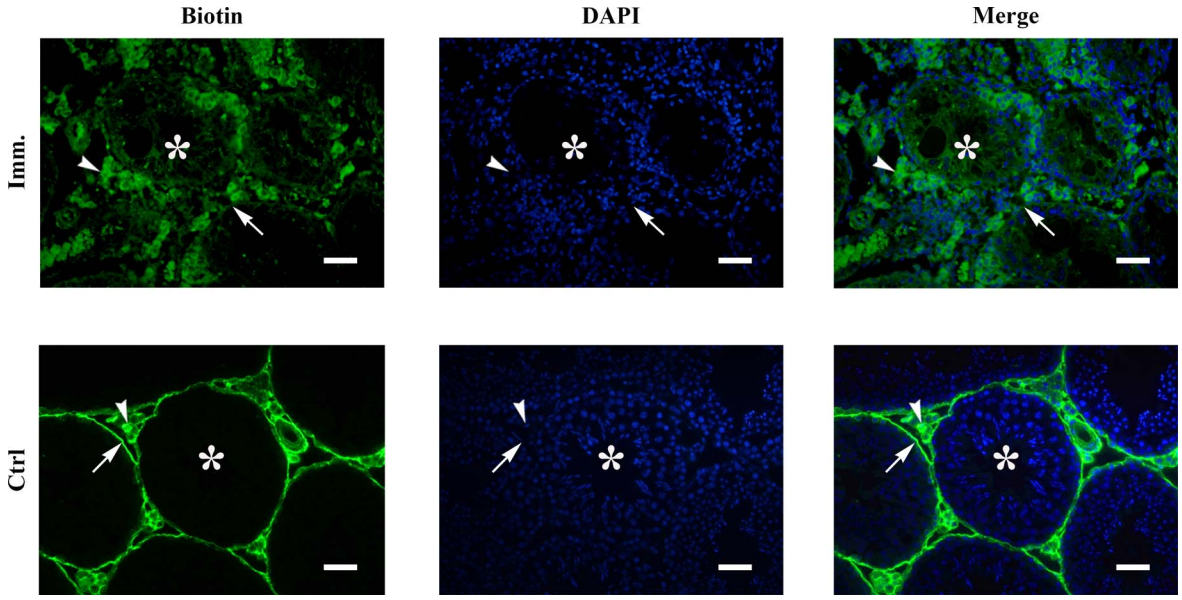

FIG. 7. BTB permeability. Biotin was injected underneath the testicular capsules of control (Ctrl) and immunized (Imm.) WT mice. After 30 min, paraffin sections were stained with FITC-conjugated streptavidin (left panels), after which the sections were counterstained with DAPI (middle panels). Images of biotin and DAPI were merged (right panels). Arrows, arrowheads, and asterisks indicate basal compartment, interstitial spaces, and adluminal compartments of seminiferous tubules, respectively. Images represent at least three experiments on three mice. Bar = 20 μm.

which TLR-initiated innate immune responses regulate antigen-specific adaptive immunity against microbial pathogens have been intensively investigated [50]. The role of TLR signaling in inducing adaptive immune response to autoantigens remains an exciting issue that merits further investigation. In this context, whether the variations in susceptibilities to EAO induction in different mouse strains are associated with their innate immune machinery should be considered.

Recent studies demonstrated that TLR2 and TLR9 are involved in EAE induction [22], whereas TLR2, TLR3, TLR4, and TLR9 are involved in EAU induction [23]. The present study showed that TLR2 and TLR4 were critical for EAO induction. These results suggest that different TLRs may be involved in the development of different autoimmune diseases, which could be associated with different autoantigens and adjuvants used in these studies. Notably, TLR2 is a common player in the three experimental autoimmune diseases models. In this study, we showed that TLR2 was critical in mediating autoantibody production in EAO. Considering that TLR2 is constitutively expressed in B cells, it should be worthwhile to clarify the role of TLR2 in regulating autoantibody generation.

In summary, the present study demonstrated that TLR2 and TLR4 were key mediators in EAO induction. Moreover, we showed that TLR2 played critical role in inducing the production of autoantibodies against male germ cell antigens in response to immunization. The data provide novel insights into the mechanisms underlying autoimmune orchitis induction.

REFERENCES

1. Yule TD, Montoya GD, Russell LD, Williams TM, Tung KS. Autoantigenic germ cells exist outside the blood testis barrier. J Immunol 1988; 141:1161–1167.
2. Schuppe HC, Meinhardt A, Allam JP, Bergmann M, Weidner W, Haidl G. Chronic orchitis: a neglected cause of male infertility? Andrologia 2008; 40:84–91.
3. Tung KS, Teuscher C. Mechanisms of autoimmune disease in the testis and ovary. Hum Reprod Update 1995; 1:35–50.
4. Itoh M, De-Rooij D, Takeuchi Y. Mode of inflammatory cell infiltration in testes of mice injected with syngeneic testicular germ cells without adjuvant. J Anat 1995; 187:671–679.
5. Jacobo P, Guazzone VA, Theas MS, Lustig L. Testicular autoimmunity. Autoimmun Rev 2011; 10:201–204.
6. Doncel GF, Di Paola JA, Lustig L. Sequential study of the histopathology and cellular and humoral immune response during the development of an autoimmune orchitis in Wistar rats. Am J Reprod Immunol 1989; 20: 44–51.
7. Jacobo P, Guazzone VA, Jarazo-Dietrich S, Theas MS, Lustig L. Differential changes in CD4+ and CD8+ effector and regulatory T lymphocyte subsets in the testis of rats undergoing autoimmune orchitis. J Reprod Immunol 2009; 81:44–54.
8. Guazzone VA, Jacobo P, Theas MS, Lustig L. Cytokines and chemokines in testicular inflammation: a brief review. Microsc Res Tech 2009; 72: 620–628.
9. Kawai T, Akira S. The role of pattern-recognition receptors in innate immunity: update on Toll-like receptors. Nat Immunol 2010; 11:373–384.
10. Kawai T, Akira S. TLR signaling. Cell Death Differ 2006; 13:816–825.
11. Yoshimura A, Lien E, Ingalls RR, Tuomanen E, Dziarski R, Golenbock D. Cutting edge: recognition of Gram-positive bacterial cell wall components by the innate immune system occurs via Toll-like receptor 2. J Immunol 1999; 163:1–5.
12. Schwandner R, Dziarski R, Wesche H, Rothe M, Kirschning CJ. Peptidoglycan- and lipoteichoic acid-induced cell activation is mediated by toll-like receptor 2. J Biol Chem 1999; 274:17406–17409.
13. Poltorak A, He X, Smirnova I, Liu MY, Van Huffel C, Du X, Birdwell D, Alejos E, Silva M, Galanos C, Freudenberg M, Ricciardi-Castagnoli P, et al. Defective LPS signaling in C3H/HeJ and C57BL/10ScCr mice: mutations in Tlr4 gene. Science 1998; 282:2085–2088.
14. Piccinini AM, Midwood KS. DAMPening inflammation by modulating TLR signalling. Mediators Inflamm 2010:672395.
15. Zetterstrom CK, Strand ML, Soder O. The high mobility group box chromosomal protein 1 is expressed in the human and rat testis where it may function as an antibacterial factor. Hum Reprod 2006; 21:2801–2809.
16. Biggiogera M, Tanguay RM, Marin R, Wu Y, Martin TE, Fakan S. Localization of heat shock proteins in mouse male germ cells: an immunoelectron microscopical study. Exp Cell Res 1996; 229:77–85.
17. Park JS, Svetkauskaite D, He Q, Kim JY, Strassheim D, Ishizaka A, Abraham E. Involvement of toll-like receptors 2 and 4 in cellular activation by high mobility group box 1 protein. J Biol Chem 2004; 279: 7370–7377.
18. Vabulas RM, Ahmad-Nejad P, da Costa C, Miethke T, Kirschning CJ, Hacker H, Wagner H. Endocytosed HSP60s use toll-like receptor 2 (TLR2) and TLR4 to activate the toll/interleukin-1 receptor signaling pathway in innate immune cells. J Biol Chem 2001; 276:31332–31339.

19. Iwasaki A, Medzhitov R. Regulation of adaptive immunity by the innate immune system. Science 2010; 327:291–295.
20. Li M, Zhou Y, Feng G, Su SB. The critical role of Toll-like receptor signaling pathways in the induction and progression of autoimmune diseases. Curr Mol Med 2009; 9:365–374.
21. Yu L, Wang L, Chen S. Endogenous toll-like receptor ligands and their biological significance. J Cell Mol Med 2010; 14:2592–2603.
22. Miranda-Hernandez S, Gerlach N, Fletcher JM, Biros E, Mack M, Korner H, Baxter AG. Role for MyD88, TLR2 and TLR9 but not TLR1, TLR4 or TLR6 in experimental autoimmune encephalomyelitis. J Immunol 2011; 187:791–804.
23. Fang J, Fang D, Silver PB, Wen F, Li B, Ren X, Lin Q, Caspi RR, Su SB. The role of TLR2, TRL3, TRL4, and TRL9 signaling in the pathogenesis of autoimmune disease in a retinal autoimmunity model. Invest Ophthalmol Vis Sci 2010; 51:3092–3099.
24. Zhao S, Zhu W, Xue S, Han D. Testicular defense systems: immune privilege and innate immunity. Cell Mol Immunol 2014; 11:428–437.
25. Jacobo P, Perez CV, Theas MS, Guazzone VA, Lustig L. CD4+ and CD8+ T cells producing Th1 and Th17 cytokines are involved in the pathogenesis of autoimmune orchitis. Reproduction 2011; 141:249–258.
26. Zhu W, Chen Q, Yan K, Liu Z, Li N, Zhang X, Yu L, Chen Y, Han D. RIG-I-like receptors mediate innate antiviral response in mouse testis. Mol Endocrinol 2013; 27:1455–1467.
27. Meng J, Holdcraft RW, Shima JE, Griswold MD, Braun RE. Androgens regulate the permeability of the blood-testis barrier. Proc Natl Acad Sci U S A 2005; 102:16696–16700.
28. Rival C, Theas MS, Suescun MO, Jacobo P, Guazzone V, van Rooijen N, Lustig L. Functional and phenotypic characteristics of testicular macrophages in experimental autoimmune orchitis. J Pathol 2008; 215: 108–117.
29. Silva CA, Cocuzza M, Carvalho JF, Bonfa E. Diagnosis and classification of autoimmune orchitis. Autoimmun Rev 2014; 13:431–434.
30. Naito M, Terayama H, Hirai S, Qu N, Lustig L, Itoh M. Experimental autoimmune orchitis as a model of immunological male infertility. Med Mol Morphol 2012; 45:185–189.
31. Fijak M, Schneider E, Klug J, Bhushan S, Hackstein H, Schuler G, Wygrecka M, Gromoll J, Meinhardt A. Testosterone replacement effectively inhibits the development of experimental autoimmune orchitis in rats: evidence for a direct role of testosterone on regulatory T cell expansion. J Immunol 2011; 186:5162–5172.
32. Kumar H, Kawai T, Akira S. Pathogen recognition by the innate immune system. Int Rev Immunol 2011; 30:16–34.
33. Chase MA, Wheeler DS, Lierl KM, Hughes VS, Wong HR, Page K. Hsp72 induces inflammation and regulates cytokine production in airway epithelium through a TLR4- and NF-kappaB-dependent mechanism. J Immunol 2007; 179:6318–6324.
34. Roelofs MF, Boelens WC, Joosten LA, Abdollahi-Roodsaz S, Geurts J, Wunderink LU, Schreurs BW, van den Berg WB, Radstake TR. Identification of small heat shock protein B8 (HSP22) as a novel TLR4 ligand and potential involvement in the pathogenesis of rheumatoid arthritis. J Immunol 2006; 176:7021–7027.
35. Asea A, Rehli M, Kabingu E, Boch JA, Bare O, Auron PE, Stevenson MA, Calderwood SK. Novel signal transduction pathway utilized by extracellular HSP70: role of toll-like receptor (TLR) 2 and TLR4. J Biol Chem 2002; 277:15028–15034.
36. Vabulas RM, Braedel S, Hilf N, Singh-Jasuja H, Herter S, Ahmad-Nejad P, Kirschning CJ, Da Costa C, Rammensee HG, Wagner H, Schild H. The endoplasmic reticulum-resident heat shock protein Gp96 activates dendritic cells via the Toll-like receptor 2/4 pathway. J Biol Chem 2002; 277:20847–20853.
37. Curtin JF, Liu N, Candolfi M, Xiong W, Assi H, Yagiz K, Edwards MR, Michelsen KS, Kroeger KM, Liu C, Muhammad AK, Clark MC, et al. HMGB1 mediates endogenous TLR2 activation and brain tumor regression. PLoS Med 2009; 6:1000010.
38. Buchta CM, Bishop GA. Toll-like receptors and B cells: functions and mechanisms. Immunol Res 2014; 59:12–22.
39. Liblau RS, Singer SM, McDevitt HO. Th1 and Th2 CD4+ T cells in the pathogenesis of organ-specific autoimmune diseases. Immunol Today 1995; 16:34–38.
40. Yule TD, Tung KS. Experimental autoimmune orchitis induced by testis and sperm antigen-specific T cell clones: an important pathogenic cytokine is tumor necrosis factor. Endocrinology 1993; 133:1098–1107.
41. Rival C, Theas MS, Guazzone VA, Lustig L. Interleukin-6 and IL-6 receptor cell expression in testis of rats with autoimmune orchitis. J Reprod Immunol 2006; 70:43–58.
42. Theas MS, Rival C, Jarazo-Dietrich S, Jacobo P, Guazzone VA, Lustig L. Tumour necrosis factor-alpha released by testicular macrophages induces apoptosis of germ cells in autoimmune orchitis. Hum Reprod 2008; 23: 1865–1872.
43. Guazzone VA, Rival C, Denduchis B, Lustig L. Monocyte chemoattractant protein-1 (MCP-1/CCL2) in experimental autoimmune orchitis. J Reprod Immunol 2003; 60:143–157.
44. Zhang X, Wang T, Deng T, Xiong W, Lui P, Li N, Chen Y, Han D. Damaged spermatogenic cells induce inflammatory gene expression in mouse Sertoli cells through the activation of Toll-like receptors 2 and 4. Mol Cell Endocrinol 2013; 365:162–173.
45. Reiling N, Holscher C, Fehrenbach A, Kroger S, Kirschning CJ, Goyert S, Ehlers S. Cutting edge: Toll-like receptor (TLR)2- and TLR4-mediated pathogen recognition in resistance to airborne infection with Mycobacterium tuberculosis. J Immunol 2002; 169:3480–3484.
46. Mendel I, Kerlero de Rosbo N, Ben-Nun A. A myelin oligodendrocyte glycoprotein peptide induces typical chronic experimental autoimmune encephalomyelitis in H-2b mice: fine specificity and T cell receptor V beta expression of encephalitogenic T cells. Eur J Immunol 1995; 25: 1951–1959.
47. Caspi RR, Silver PB, Luger D, Tang J, Cortes LM, Pennesi G, Mattapallil MJ, Chan CC. Mouse models of experimental autoimmune uveitis. Ophthalmic Res 2008; 40:169–174.
48. Segal BM, Chang JT, Shevach EM. CpG oligonucleotides are potent adjuvants for the activation of autoreactive encephalitogenic T cells in vivo. J Immunol 2000; 164:5683–5688.
49. Li N, Liu Z, Zhang Y, Chen Q, Liu P, Cheng CY, Lee WM, Chen Y, Han D. Mice lacking Axl and Mer tyrosine kinase receptors are susceptible to experimental autoimmune orchitis induction. Immunol Cell Biol (in press). Published online ahead of print 18 November 2014; DOI: 10.1038/icb. 2014.97.
50. Schenten D, Medzhitov R. The control of adaptive immune responses by the innate immune system. Adv Immunol 2011; 109:87–124.